

Parameters estimation and uncertainty assessment in the transmission dynamics of rabies in humans and dogs

Mfano Charles^{a,b,*}, Sayoki G. Mfinanga^c, G.A. Lyakurwa^a, Delfim F. M. Torres^d, Verdiana G. Masanja^a

^a*School of Computational and Communication Science and Engineering,
Nelson Mandela African Institution of Science and Technology (NM-AIST), P.O. Box 447, Arusha, Tanzania*
^b*Department of ICT and Mathematics, College of Business Education (CBE), P.O. BOX 1968 Dar es Salaam, Tanzania*
^c*NIMR Chief Research Scientist Fellow*
^d*Center for Research and Development in Mathematics and Applications (CIDMA),
Department of Mathematics, University of Aveiro, 3810-193 Aveiro, Portugal*

Abstract

Rabies remains a pressing global public health issue, demanding effective modeling and control strategies. This study focused on developing a mathematical model using ordinary differential equations (ODEs) to estimate parameters and assess uncertainties related to the transmission dynamics of rabies in humans and dogs. To determine model parameters and address uncertainties, next-generation matrices were utilized to calculate the basic reproduction number \mathcal{R}_0 . Furthermore, the Partial Rank Correlation Coefficient was used to identify parameters that significantly influence model outputs. The analysis of equilibrium states revealed that the rabies-free equilibrium is globally asymptotically stable when $R_0 < 1$, whereas the endemic equilibrium is globally asymptotically stable when $\mathcal{R}_0 \geq 1$. To reduce the severity of rabies and align with the Global Rabies Control (GRC) initiative by 2030, the study recommends implementing control strategies targeting indoor domestic dogs.

Keywords: Rabies dynamics, Mathematical Modeling, Latin Hypercube Sampling (LHS), Contact rate, Parameter uncertainty.

1. Introduction

Rabies is a fatal and neglected viral disease that affects mammals, including humans. The disease is primarily spread through bites and scratches by infected animals [1, 2, 3, 4, 5]. The disease is caused by rabies virus, a member of the family Rhabdoviridae and the genus Lyssavirus. The disease typically presents with symptoms such as inflammation, fever, headache, and malaise. These initial symptoms can progress to more specific manifestations including anxiety, confusion, hallucinations, dysphagia, muscle spasms, and paralysis, therefore, immediate medical attention is essential in the event of a bite or scratch from animals such as dogs and cats [6, 7, 8, 9]. Prevention of rabies primarily involves vaccinating humans and domestic dogs, and avoiding contact with wild animals that are carriers of rabies virus [2, 10]. In many countries, vaccination programs have been successful in reducing the incidence of rabies in humans and domestic dogs [11, 12]. Post-exposure prophylaxis (PEP) is a vaccine recommended for individuals who have been bitten or scratched by an animal who are carrier of rabies virus. PEP comprises a series of injections with both rabies vaccine and rabies immune globulin to prevent the virus from causing an infection [3].

Mathematical models are fundamental tools for comprehending and addressing the transmission dynamics of rabies. They aid in describing and predicting epidemiological phenomena, allocating resources, and structuring control strategies. Researchers in different countries have developed several mathematical models

*Corresponding author

Email addresses: mfanoc@nm-aist.ac.tz (Mfano Charles), gsmfinanga@yahoo.com (Sayoki G. Mfinanga), geminpeter.lyakurwa@nm-aist.ac.tz (G.A. Lyakurwa), delfim@ua.pt (Delfim F. M. Torres), verdiana.masanja@nm-aist.ac.tz (Verdiana G. Masanja)

to study the transmission dynamics of rabies in dog populations [13, 14, 15, 16, 17, 18], as well as interactions between dog and human populations [19, 20, 21], and even among dog, human, and other animal populations [22, 23, 24]. These studies have identified several factors that can shape the dynamics of rabies in different countries and ways of controlling the disease. However, due to the complex nature of disease transmission dynamics and the inherent variability in real-world data, parameter estimation poses significant challenges. Estimating these parameters accurately is essential for designing effective control measures and interventions to prevent the spread of rabies. One common approach to parameter estimation involves using the least square method and validating the model by fitting real-world data to the proposed model. It is crucial to assess uncertainty in parameter estimates to understand the reliability of model predictions and make informed decisions about disease control strategies. Uncertainty can arise from various sources, including variability in data, model structure, and parameter estimation techniques.

To address this issue, statistical techniques such as Latin Hypercube Sampling (LHS) and Partial Rank Correlation Coefficient (PRCC) are utilized for uncertainty and sensitivity analysis of input parameters [25]. LHS generates random samples within the parameter space, while PRCC assesses the correlation between model output and each input parameter [25, 26]. LHS enables efficient sampling of multi-dimensional parameter space, while PRCC computes and ranks the correlation coefficient between the model inputs (parameters) and the model outputs (state variables). It gauges the degree of a non-linear and monotonic relationship between model inputs (parameters) and model outputs. Therefore, this paper discusses the transmission dynamics of rabies, the parameter estimation, and the role of statistical techniques such as LHS and PRCC in evaluating the impact of uncertainties on model predictions.

The structure of this paper is organized with sections dedicated to formulating the mathematical model (Section 2), qualitative analysis (Section 3), quantitative analysis (Section 4), and discussion and concluding the findings (Sections 5 and 6, respectively).

2. Model Formulation

The model for rabies transmission is divided into four distinctive components. The first component pertains to the human population, which is represented by $N_H = S_H + E_H + R_H + I_H$. The second component is the environmental virus reservoir, represented by M . The third component is comprised of free-range dogs, represented by $N_F = S_F + E_F + I_F$, which includes both stray and feral dogs. The fourth component represents domestic dogs, represented by $N_D = S_D + E_D + R_D + I_D$. Susceptible humans (S_H) are individuals who can be infected. They are recruited into the population at a rate of θ_1 . Exposure happens upon contact with infected free-range dogs (I_F), domestic dogs (I_D), or the virus (M) at rates of τ_1 , τ_2 , or τ_3 , respectively. The latency period for exposed individuals is 1-3 months. Thus the force of infection for human is given by

$$\chi_1 = (\tau_1 I_F + \tau_2 I_D + \tau_3 \lambda(M)) S_H, \quad (1)$$

where

$$\lambda(M) = \frac{M}{M + C}.$$

Exposed individuals who receive post-exposure prophylaxis recover at a rate of β_2 . Vaccinated individuals lose their protective immunity and become susceptible at a rate of β_3 . In some cases, exposed individuals vaccinated with less efficacious vaccine may progress to infectious state I_H at the transition rate of β_1 . Infected individuals may suffer to induced deaths at a rate of σ_1 . Susceptible free-range dogs S_F become infected upon contact with infected individuals I_F , I_D , or the rabies virus in the environment at rates of κ_1 , κ_2 , or κ_3 , respectively. The force of infection of free range dogs is given by

$$\chi_2 = (\kappa_1 I_F + \kappa_2 I_D + \kappa_3 \lambda(M)) S_F. \quad (2)$$

Upon exposure to rabies, susceptible free-range dogs transition to the latent state E_F , where they remain for 1 to 3 months. Subsequently, they advance to the infectious state I_F at a rate γ . Infected free-range dogs face mortality at a rate σ_2 , while all free-range dogs experience natural death at a rate of μ_2 .

Susceptible domestic dogs (S_D) are continually recruited at a rate θ_3 and become infected through contact with either infected individuals (I_F , I_D , M) or the virus in the environment at rates ψ_1 , ψ_2 , or ψ_3 , respectively, and the force of infection is defined as

$$\chi_3 = \left(\frac{\psi_1 I_F}{1 + \rho_1} + \frac{\psi_2 I_D}{1 + \rho_2} + \frac{\psi_3}{1 + \rho_3} \lambda(M) \right) S_D. \quad (3)$$

Following exposure to rabies, susceptible domestic dogs transition to the latent state E_D , where they remain for a period of time at a rate β_1 . Those in E_D who receive post-exposure prophylaxis move to the recovered state R_D at rate γ_2 . However, as post-exposure prophylaxis does not provide permanent immunity, individuals in R_D can lose immunity and become susceptible again at rate γ_3 . The remaining portion of E_D progresses to the infectious state I_D at rate γ_1 . Infected domestic dogs face mortality due to the disease at rate σ_3 . Additionally, all domestic dogs experience natural death at a rate of μ_3 . The rabies virus in the environment is introduced through shedding from infectious free-range dogs, domestic dogs, and humans at rates ν_2 , ν_3 , and ν_1 , respectively, at the general rate defined as

$$\theta_4 = (\nu_1 I_H + \nu_2 I_F + \nu_3 I_D) M. \quad (4)$$

The viruses are eliminated from the environment at a rate of μ_4 .

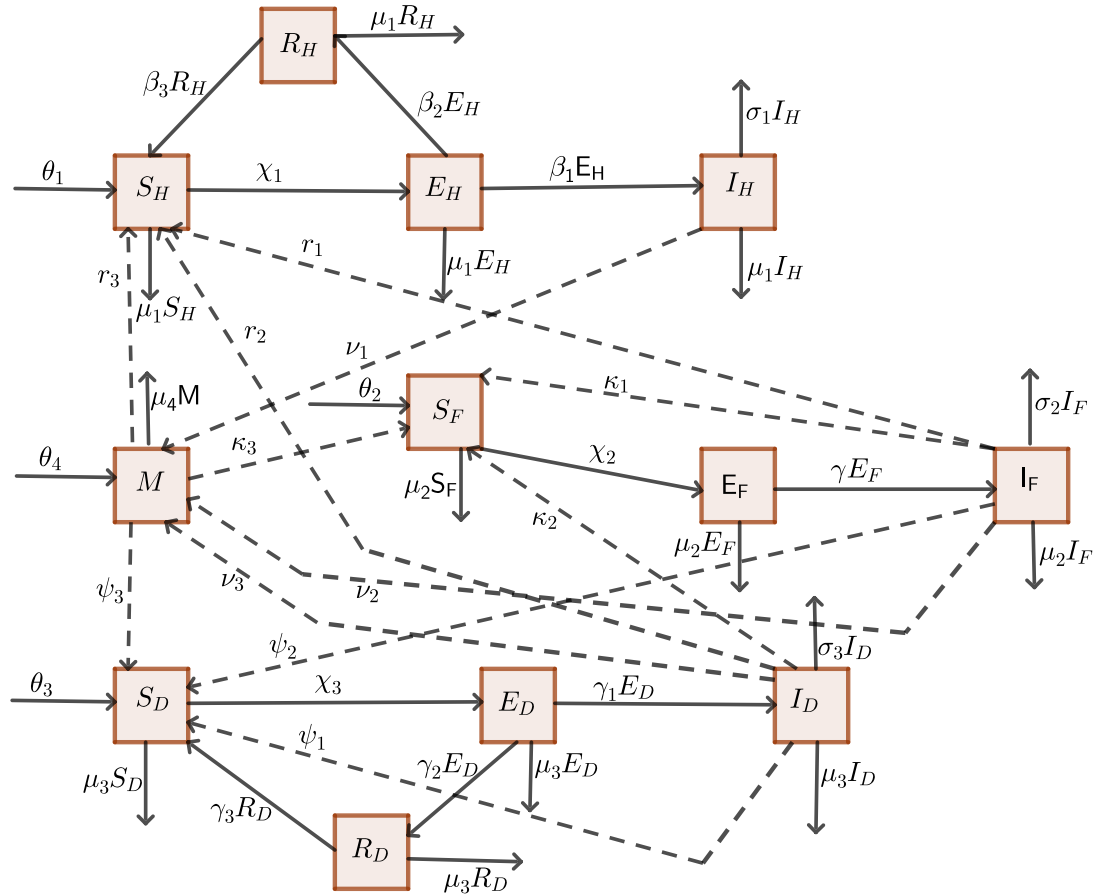


Figure 1: Schematic diagram for the flow of transmission dynamics of rabies.

Using the details provided about the model parameters and their associations with the state variables,

we develop a model represented as a set of ordinary differential equations, as shown in equation (5),

$$\begin{cases} \dot{S}_H &= \theta_1 + \beta_3 R_H - \chi_1 - \mu_1 S_D, \\ \dot{E}_H &= \chi_2 - (\mu_1 + \beta_1 + \beta_2) E_H, \\ \dot{I}_H &= \beta_1 E_H - (\sigma_1 + \mu_1) I_H, \\ \dot{R}_H &= \beta_2 E_H - (\beta_3 + \mu_1) R_H, \\ \dot{S}_F &= \theta_2 - \chi_2 - \mu_2 S_F, \\ \dot{E}_F &= \chi_2 - (\mu_2 + \gamma) E_F, \\ \dot{I}_F &= \gamma E_F - (\mu_2 + \sigma_2) I_F, \\ \dot{S}_D &= \theta_3 - \chi_3 - \mu_3 S_D + \gamma_3 R_D, \\ \dot{E}_D &= \chi_3 - (\mu_3 + \gamma_1 + \gamma_2) E_D, \\ \dot{I}_D &= \gamma_1 E_D - (\mu_3 + \sigma_3) I_D, \\ \dot{R}_D &= \gamma_2 E_D - (\mu_3 + \gamma_3) R_D, \\ \dot{M} &= (\nu_1 I_H + \nu_2 I_F + \nu_3 I_D) - \mu_4 M, \end{cases} \quad (5)$$

subject to the following non-negative conditions:

$$\begin{aligned} S_H(0) > 0, E_H(0) \geq 0, I_H(0) \geq 0, R_H(0) \geq 0, \quad S_F(0) > 0, E_F(0) \geq 0, I_F(0) \geq 0, \\ S_D(0) \geq 0, E_D(0) \geq 0, I_D(0) \geq 0, R_D(0) \geq 0. \end{aligned} \quad (6)$$

The schematic diagram corresponding to (5) is given in Fig. 1.

3. Qualitative analysis

In this section we prove existence of a positive solution, its boundedness, we compute the Rabies free equilibrium and the basic reproduction number.

3.1. Positivity of the solution

For the model system (5) to be epidemiologically meaningfully and well-posed, we need to prove that the state variables are non-negative $\forall t \geq 0$.

Lemma 1. *All solution of the system in the region (5) that start in $\Omega \subset \mathbb{R}_+^{12}$ remain positive all the time.*

Proof. To prove for the existence of model solution (5), we consider initial conditions and apply the integral

operator $\int_0^t (\cdot) ds$ to all equations in the model equation (5), to obtain:

$$\left\{ \begin{array}{l} S_H(t) - S_H(0) = \int_0^t (\theta_1 + \beta_3 R_H - \mu_1 S_H - \chi_1) ds, \\ E_H(t) - E_H(0) = \int_0^t (\chi_1 - (\mu_1 + \beta_1 + \beta_2) E_H) ds, \\ I_H(t) - I_H(0) = \int_0^t (\beta_1 E_H - (\sigma_1 + \mu_1) I_H) ds, \\ R_H(t) - R_H(0) = \int_0^t (\beta_2 E_H - (\beta_3 + \mu_1) R_H) ds, \\ \\ S_F(t) - S_F(0) = \int_0^t (\theta_2 - \chi_2 - \mu_2 S_F) ds, \\ E_F(t) - E_F(0) = \int_0^t (\chi_2 - (\mu_2 + \gamma) E_F) ds, \\ I_F(t) - I_F(0) = \int_0^t (\gamma E_F - (\mu_2 + \sigma_2) I_F) ds, \\ \\ S_D(t) - S_D(0) = \int_0^t (\theta_3 - \mu_3 S_D - \chi_3 + \gamma_3 R_D) ds, \\ E_D(t) - E_D(0) = \int_0^t (\chi_3 - (\mu_3 + \gamma_1 + \gamma_2) E_D) ds, \\ I_D(t) - I_D(0) = \int_0^t (\gamma_1 E_D - (\mu_3 + \sigma_3) I_D) ds, \\ R_D(t) - R_D(0) = \int_0^t (\gamma_2 E_D - (\mu_3 + \gamma_3) R_D) ds, \\ \\ M(t) - M(0) = \int_0^t ((\nu_1 I_H + \nu_2 I_F + \nu_3 I_D) - \mu_4 M) ds. \end{array} \right. \quad (7)$$

For convenience, from equation (7) we define the following functions:

$$\left\{ \begin{array}{l} f_1(t, S_H) = \theta_1 + \beta_3 R_H - \mu_1 S_H - \chi_1, \\ f_2(t, E_H) = \chi_1 - (\mu_1 + \beta_1 + \beta_2 + u_4) E_H, \\ f_3(t, E_H) = \beta_1 E_H - (\sigma_1 + \mu_1) I_H, \\ f_4(t, R_H) = (\beta_2 + u_4) E_H - (\beta_3 + \mu_1) R_H, \\ \\ f_5(t, S_F) = \theta_2 - \chi_2 - \mu_2 S_F, \\ f_6(t, E_F) = \chi_2 - (\mu_2 + \gamma) E_F, \\ f_7(t, I_F) = \gamma E_F - (\mu_2 + \sigma_2) I_F, \\ \\ f_8(t, S_D) = \theta_3 - \mu_3 S_D - \chi_3 + \gamma_3 R_D, \\ f_9(t, E_D) = \chi_3 - (\mu_3 + \gamma_1 + \gamma_2) E_D, \\ f_{10}(t, I_D) = \gamma_1 E_D - (\mu_3 + \sigma_3) I_D, \\ f_{11}(t, R_D) = \gamma_2 E_D - (\mu_3 + \gamma_3) R_D, \\ \\ f_{12}(t, M) = (\nu_1 I_H + \nu_2 I_F + \nu_3 I_D) - \mu_4 M. \end{array} \right. \quad (8)$$

Since $S_H, E_H, I_H, R_H, S_F, E_F, I_F, S_D, E_D, I_D, R_D, M$ are positive and bounded in the region $\Omega \subset \mathbb{R}_+^{12}$, there exists non-negative values $\mathbb{L}_i, i = 1, 2, \dots, 12$, such that

$$\begin{aligned}
\|f_1(t, S_H(t)) - f_1(t, S_H(t)_1)\| &\leq \|(\theta_1 + \beta_3 R_H(t) - \mu_1 S_H(t) - \chi_1(t)) \\
&\quad - (\theta_1 + \beta_3 R_H(t) - \mu_1 S_H(t)_1 - \chi_1(t))_1\| \\
&\leq \mu_1 \|S_H(t)_1 - S_H(t)\| + \chi_1 \|S_H(t)_1 - S_H(t)\| \quad (9) \\
&\leq (\mu_1 + \chi_1) \|S_H(t)_1 - S_H(t)\| \\
&\leq \epsilon_1 \|S_H(t)_1 - S_H(t)\|.
\end{aligned}$$

Using similar approach as used in equation (9) we obtain for functions f_i , $i = 2, 3, \dots, 12$, that

$$\left\{ \begin{array}{l}
\|f_2(t, E_H(t)) - f_2(t, E_H(t)_1)\| \leq \epsilon_2 \|E_H(t)_1 - E_H(t)\|, \\
\|f_3(t, I_H(t)) - f_3(t, I_H(t)_1)\| \leq \epsilon_3 \|I_H(t)_1 - I_H(t)\|, \\
\|f_4(t, R_H(t)) - f_4(t, R_H(t)_1)\| \leq \epsilon_4 \|R_H(t)_1 - R_H(t)\|, \\
\|f_5(t, S_F(t)) - f_5(t, S_F(t)_1)\| \leq \epsilon_5 \|S_F(t)_1 - S_F(t)\|, \\
\|f_6(t, E_F(t)) - f_6(t, E_F(t)_1)\| \leq \epsilon_6 \|E_F(t)_1 - E_F(t)\|, \\
\|f_7(t, I_F(t)) - f_7(t, I_F(t)_1)\| \leq \epsilon_7 \|I_F(t)_1 - I_F(t)\|, \quad (10) \\
\|f_8(t, S_D(t)) - f_8(t, S_D(t)_1)\| \leq \epsilon_8 \|S_D(t)_1 - S_D(t)\|, \\
\|f_9(t, E_D(t)) - f_9(t, E_D(t)_1)\| \leq \epsilon_9 \|E_D(t)_1 - E_D(t)\|, \\
\|f_{10}(t, I_D(t)) - f_{10}(t, I_D(t)_1)\| \leq \epsilon_{10} \|I_D(t)_1 - I_D(t)\|, \\
\|f_{11}(t, S_D(t)) - f_{11}(t, R_D(t)_1)\| \leq \epsilon_{11} \|R_D(t)_1 - R_D(t)\|, \\
\|f_{12}(t, M(t)) - f_{12}(t, M(t)_1)\| \leq \epsilon_{12} \|M(t)_1 - M(t)\|,
\end{array} \right.$$

where $\epsilon_1 = \mu_1 + \chi_1$, $\epsilon_2 = \mu_1 + \beta_1 + \beta_2 + u_4$, $\epsilon_3 = \sigma_1 + \mu_1$, $\epsilon_4 = \beta_3 + \mu_1$, $\epsilon_5 = \mu_2 + \chi_2$, $\epsilon_6 = \mu_2 + \gamma$, $\epsilon_7 = \mu_2 + \sigma_1$, $\epsilon_8 = \mu_3 + \chi_3$, $\epsilon_9 = \mu_3 + \gamma_1 + \gamma_2 + u_4$, $\epsilon_{10} = \mu_3 + \sigma_3$, $\epsilon_{11} = \mu_3 + \gamma_3$, $\epsilon_{12} = \mu_4$. Since the Lipschitz condition is satisfied, then a solution to our model (5) exists. \square

3.2. Boundedness of the model solution

Theorem 2. *The solution of the rabies model system (5) is uniformly bounded if $\Omega \in \mathbb{R}_+^{12}$ and $\Omega = \Omega_H \cup \Omega_D \cup \Omega_F \cup \Omega_M \in \mathbb{R}_+^4 \times \mathbb{R}_+^3 \times \mathbb{R}_+^4 \times \mathbb{R}_+^1$, where*

$$\begin{aligned}
\Omega_H &= \left\{ (S_H, E_H, I_H, R_H) \in \mathbb{R}_+^4 : 0 \leq N_H \leq \frac{\theta_1}{\mu_1} \right\}, \quad \Omega_F = \left\{ (S_F, E_F, I_F) \in \mathbb{R}_+^3 : 0 \leq N_F \leq \frac{\theta_2}{\mu_2} \right\}, \\
\Omega_D &= \left\{ (S_D, E_D, I_D, R_D) \in \mathbb{R}_+^4 : 0 \leq N_D \leq \frac{\theta_3}{\mu_3} \right\}, \quad \Omega_M = \max \left\{ \frac{\theta_1 \nu_1}{\mu_1 \mu_4} + \frac{\theta_2 \nu_2}{\mu_2 \mu_4} + \frac{\theta_3 \nu_3}{\mu_3 \mu_4}, M(0) \right\},
\end{aligned}$$

and Ω is the positive invariant region.

Proof. Since the model (5) monitors both human and dog populations, we assume that the model's state variables and parameters are non-negative for all $t \geq 0$. By utilizing Theorem 2, we derive the invariant region of the rabies model as follows. Consider the population of the human from equation (5) as

$$\frac{dN_H}{dt} = \frac{dS_H}{dt} + \frac{dE_H}{dt} + \frac{dI_H}{dt} + \frac{dR_H}{dt}. \quad (11)$$

Then, equation (11) implies to equation (12) as follows:

$$\frac{dN_H}{dt} = \theta_1 - (S_H + E_H + I_H + R_H) \mu_1 - \sigma_1 I_H. \quad (12)$$

But if $N_H = S_H + E_H + I_H + R_H$, then Equation (12) can be written as

$$\frac{dN_H}{dt} = \theta_1 - N_H \mu_1, \quad (13)$$

and by utilizing the integrating factor in equation (13) and $t \rightarrow 0$, we have

$$N_H(0) \leq \frac{\theta_1}{\mu_1} + Ce^0 \implies N_H(0) - \frac{\theta_1}{\mu_1} \leq C. \quad (14)$$

By simplifying equation (14) and after simple manipulations, it follows that

$$\Omega_H = \left\{ (S_H, E_H, I_H, R_H) \in \mathbb{R}_+^4 : 0 \leq N_H \leq \frac{\theta_1}{\mu_1} \right\}.$$

Employing the same procedures for free range and domestic dog populations, we obtain:

$$\Omega_F = \left\{ (S_F, E_F, I_F) \in \mathbb{R}_+^3 : 0 \leq N_F \leq \frac{\theta_2}{\mu_2} \right\}, \quad \Omega_D = \left\{ (S_D, E_D, I_D, R_D) \in \mathbb{R}_+^4 : 0 \leq N_D \leq \frac{\theta_3}{\mu_3} \right\}. \quad (15)$$

Again, from the environment that contains rabies virus,

$$\dot{M} = (\nu_1 I_H + \nu_2 I_F + \nu_3 I_D) - \mu_4 M. \quad (16)$$

Since $N_H \leq \frac{\theta_1}{\mu_1}$, $N_F \leq \frac{\theta_2}{\mu_2}$, and $N_D \leq \frac{\theta_3}{\mu_3}$, it follows that $I_H \leq \frac{\theta_1}{\mu_1}$, $I_F \leq \frac{\theta_2}{\mu_2}$, and $I_D \leq \frac{\theta_3}{\mu_3}$. Therefore, Equation (16) can be expressed as

$$\dot{M} \leq \left(\frac{\nu_1 \theta_1}{\mu_1} + \frac{\nu_2 \theta_2}{\mu_2} + \frac{\nu_3 \theta_3}{\mu_3} \right) - \mu_4 M. \quad (17)$$

Now, let Y be the solution which is unique to the initial value problem such that

$$\left. \begin{aligned} \dot{Y} &\leq \left(\frac{\nu_1 \theta_1}{\mu_1} + \frac{\nu_2 \theta_2}{\mu_2} + \frac{\nu_3 \theta_3}{\mu_3} \right) - \mu_4 Y, \quad \text{for } t > 0 \\ Y(0) &= M(0). \end{aligned} \right\} \quad (18)$$

By using integration factor equation (18) as $t \rightarrow \infty$, we get the expression

$$\left(M(0) - \left(\frac{\nu_1 \theta_1}{\mu_1} + \frac{\nu_2 \theta_2}{\mu_2} + \frac{\nu_3 \theta_3}{\mu_3} \right) \frac{1}{\mu_4} e^{\mu_4 t} \right) \quad (19)$$

and as equation (19) goes to zero, we have

$$M(t) \leq \Omega_M. \quad (20)$$

Thus, the model system (5) is biologically and mathematically meaningful such that their solution relies in the region Ω . \square

3.3. Rabies free equilibrium (\mathbb{E}_0) and the basic reproduction number \mathcal{R}_0

In order to achieve a rabies-free equilibrium (\mathbb{E}_0) in both humans, free-range, and domestic dog populations, we equate all infectious compartments in equation (5) to zero, which leads to

$$\mathbb{E}_0 = \left(\frac{\theta_1}{\mu_1}, 0, 0, 0, \frac{\theta_2}{\mu_2}, 0, 0, \frac{\theta_3}{\mu_3}, 0, 0, 0, 0 \right).$$

In order to determine the basic reproduction \mathcal{R}_0 , the next generation matrix method, as applied by [27, 28, 29], is adopted as follows:

$$\frac{dx_i}{dt} = \mathcal{F}_i(x) - (\mathcal{V}_i^+(x) - \mathcal{V}_i^-(x)), \quad (21)$$

where \mathcal{F}_i is the matrix new infections in the compartment i while \mathcal{V}_i^+ and \mathcal{V}_i^- are matrices of the transfer terms in and out of the compartment i , respectively. From equation (21), we define \mathcal{F}_i and \mathcal{V}_i by

$$\mathcal{F}_i = \begin{pmatrix} (\tau_1 I_F + \tau_2 I_D + \tau_3 \lambda(M)) S_H \\ 0 \\ (\kappa_1 I_F + \kappa_2 I_D + \kappa_3 \lambda(M)) S_F \\ 0 \\ \left(\frac{\psi_1 I_F}{1+\rho_1} + \frac{\psi_2 I_D}{1+\rho_2} + \frac{\psi_3}{1+\rho_3} \lambda(M) \right) S_D \\ 0 \\ 0 \end{pmatrix}, \quad \mathcal{V}_i = \begin{pmatrix} (\mu_1 + \beta_1 + \beta_2) E_H \\ (\sigma_1 + \mu_1) I_H - \beta_1 E_H \\ (\mu_2 + \gamma) E_F \\ (\mu_2 + \sigma_2) I_F - \gamma E_F \\ (\mu_3 + \gamma_1 + \gamma_2) E_D \\ (\mu_3 + \delta_3) I_D - \gamma_1 E_D \\ \mu_4 M - (\nu_1 I_H + \nu_2 I_F + \nu_3 I_D) \end{pmatrix}. \quad (22)$$

The Jacobian matrices F and V at the disease free equilibrium point \mathbb{E}_0 are given by the expression of matrix FV^{-1} which can be presented as

$$FV^{-1} = \begin{pmatrix} 0 & 0 & R_{13} & R_{14} & R_{15} & R_{16} & 0 \\ 0 & 0 & 0 & 0 & 0 & 0 & 0 \\ 0 & 0 & R_{33} & R_{34} & R_{35} & R_{36} & 0 \\ 0 & 0 & 0 & 0 & 0 & 0 & 0 \\ 0 & 0 & R_{53} & R_{54} & R_{55} & R_{56} & 0 \\ 0 & 0 & 0 & 0 & 0 & 0 & 0 \\ 0 & 0 & 0 & 0 & 0 & 0 & 0 \end{pmatrix}, \quad (23)$$

where

$$\left. \begin{aligned} R_{13} &= \frac{\tau_1 \theta_1 \gamma}{\mu_1 (\mu_2 + \gamma) (\mu_2 + \sigma_2)}, & R_{14} &= \frac{\tau_1 \theta_1}{\mu_1 (\mu_2 + \sigma_2)}, & R_{15} &= \frac{\tau_2 \theta_1 \gamma}{\mu_1 (\mu_3 + \gamma_1 + \gamma_2) (\mu_3 + \sigma_3)}, \\ R_{33} &= \frac{\kappa_1 \theta_2 \gamma}{\mu_2 (\mu_2 + \gamma) (\mu_2 + \sigma_2)}, & R_{34} &= \frac{\kappa_1 \theta_2}{\mu_2 (\mu_2 + \sigma_2)}, & R_{35} &= \frac{\kappa_1 \theta_2 \gamma}{\mu_2 (\mu_3 + \gamma_1 + \gamma_2) (\mu_3 + \sigma_3)}, \\ R_{53} &= \frac{\psi_1 \theta_3 \gamma}{(1 + \rho_1) (\mu_2 + \gamma) (\mu_2 + \sigma_2) \mu_3}, & R_{54} &= \frac{\psi_1 \theta_3}{(1 + \rho_1) \mu_3 (\mu_2 + \sigma_2)}, & R_{16} &= \frac{\tau_2 \theta_1}{\mu_1 (\mu_3 + \sigma_3)}, \\ R_{55} &= \frac{\psi_2 \theta_3 \gamma}{(1 + \rho_2) (\mu_3 + \gamma_1 + \gamma_2) (\mu_3 + \sigma_3) \mu_3}, & R_{56} &= \frac{\psi_2 \theta_3}{(1 + \rho_2) \mu_3 (\mu_3 + \sigma_3)}, & R_{36} &= \frac{\kappa_1 \theta_2}{\mu_2 (\mu_3 + \sigma_3)}. \end{aligned} \right\} \quad (24)$$

From equation (23), we obtain the eigenvalues as

$$\left(0, 0, 0, 0, 0, \frac{1}{2} R_{55} + \frac{1}{2} R_{33} + \frac{1}{2} \sqrt{R_{33}^2 - 2R_{33}R_{55} + 4R_{35}R_{53} + R_{55}^2}, \right. \\ \left. \frac{1}{2} R_{55} + \frac{1}{2} R_{33} - \frac{1}{2} \sqrt{R_{33}^2 - 2R_{33}R_{55} + 4R_{35}R_{53} + R_{55}^2} \right). \quad (25)$$

This non-negative eigenvalue corresponds to a non-negative eigenvector that represents the distribution of infected individuals who generate the highest number of secondary infections per generation, also known as \mathcal{R}_0 . According to [30], the basic reproduction number \mathcal{R}_0 is the largest eigenvalue of the next generating matrix given by

$$\mathcal{R}_0 = \rho(FV^{-1}). \quad (26)$$

Therefore, the spectral radius of the next generation matrix is given by

$$\mathcal{R}_0 = \rho(FV^{-1}) = \frac{(R_{55} + R_{33}) + \sqrt{R_{33} (R_{33} - 2R_{55}) + 4R_{35}R_{53} + R_{55}^2}}{2}. \quad (27)$$

3.3.1. Global stability of the Rabies free equilibrium

The model behaviour at the disease free equilibrium point, \mathbb{E}_0 , is investigated using a Metzler matrix as applied by Castillo-Chavez et al. [31]. Let X_s denote non-transmitting class, X_m be transmitting class and

X_{DFE} be the Disease Free equilibrium, whereby

$$\left. \begin{aligned} \frac{dX_s}{dt} &= B(X_s - X_{DFE}) + B_1 X_m \\ \frac{dX_m}{dt} &= B_2 X_m \end{aligned} \right\}. \quad (28)$$

Then, from the model system (5), it can be deduced that

$$X_s = (S_H, R_H, S_F, S_D, R_D)^T, \quad X_m = (E_H, I_H, E_D, I_D, M)^T,$$

$$X_s - X_{DFE} = \begin{bmatrix} S_H - \frac{\theta_1}{\mu_1} \\ R_H \\ S_F - \frac{\theta_2}{\mu_2} \\ S_D - \frac{\theta_3}{\mu_3} \\ R_D \end{bmatrix}, \quad B = \begin{bmatrix} -\mu & \beta_3 & 0 & 0 & 0 \\ 0 & -(\beta_3 + \mu_1) & 0 & 0 & 0 \\ 0 & 0 & -\mu_2 & 0 & 0 \\ 0 & 0 & 0 & -\mu_3 & \gamma_3 \\ 0 & 0 & 0 & 0 & -(\mu_3 + \gamma_3) \end{bmatrix},$$

$$B_1 = \begin{bmatrix} 0 & 0 & 0 & \frac{\tau_1 \theta_1}{\mu_1} & 0 & \frac{\tau_2 \theta_1}{\mu_1} & 0 \\ \beta_2 & 0 & 0 & 0 & 0 & 0 & 0 \\ 0 & 0 & 0 & \frac{\kappa_1 \theta_2}{\mu_2} & 0 & \frac{\kappa_2 \theta_2}{\mu_2} & 0 \\ 0 & 0 & 0 & \frac{\psi_1 \theta_3}{\mu_3(1+\rho_1)} & 0 & \frac{\psi_2 \theta_3}{\mu_3(1+\rho_2)} & 0 \\ 0 & 0 & 0 & 0 & \gamma_2 & 0 & 0 \end{bmatrix}, \quad \text{and}$$

$$B_2 = \begin{bmatrix} -\mu_1 - \beta_1 - \beta_2 & 0 & 0 & \frac{\tau_1 \theta_1}{\mu_1} & 0 & \frac{\tau_2 \theta_1}{\mu_1} & 0 \\ \beta_1 & -\sigma_1 - \mu_1 & 0 & 0 & 0 & 0 & 0 \\ 0 & 0 & -\mu_2 - \gamma & \frac{\kappa_1 \theta_2}{\mu_2} & 0 & \frac{\kappa_2 \theta_2}{\mu_2} & 0 \\ 0 & 0 & \gamma & -\mu_2 - \sigma_2 & 0 & 0 & 0 \\ 0 & 0 & 0 & \frac{\psi_1 \theta_3}{\mu_3(1+\rho_1)} & -\mu_3 - \gamma_1 - \gamma_2 & \frac{\psi_2 \theta_3}{\mu_3(1+\rho_1)} & 0 \\ 0 & 0 & 0 & 0 & \gamma & -\mu_3 - \sigma_3 & 0 \\ 0 & \nu_1 & 0 & \nu_2 & 0 & \nu_3 & -\mu_4 \end{bmatrix}.$$

The non-negative out-diagonal entries of matrix B_2 indicate that it is the Metzler matrix. To prove the stability of matrix B_2 using the Metzler matrix block form, we need to demonstrate that it satisfies the conditions for a Metzler matrix and has eigenvalues with negative real parts. We adopt the idea of a stable Metzler matrix and apply the following Lemma 3.

Lemma 3 (See [32]). *Let N be a square Metzler matrix written in block form*

$$N = \begin{bmatrix} A & B \\ C & D \end{bmatrix}, \quad (29)$$

where A , B and D are rectangular matrices while C is a square matrix. Then N is Metzler stable if, and only if, matrices A and $D - CA^{-1}B$ are Metzler stable.

In our case one has

$$A = \begin{bmatrix} -\mu_1 - \beta_1 - \beta_2 & 0 & 0 \\ \beta_1 & -\sigma_1 - \mu_1 & 0 \\ 0 & 0 & -\mu_2 - \gamma \end{bmatrix}, B = \begin{bmatrix} \frac{\tau_1 \theta_1}{\mu_1} & 0 & \frac{\tau_2 \theta_1}{\mu_1} & 0 \\ 0 & 0 & 0 & 0 \\ \frac{\kappa_1 \theta_2}{\mu_2} & 0 & \frac{\kappa_1 \theta_2}{\mu_2} & 0 \\ 0 & 0 & 0 & 0 \\ \frac{\psi_1 \theta_3}{\mu_3(1+\rho_1)} & 0 & \frac{\psi_2 \theta_3}{\mu_3(1+\rho_1)} & 0 \\ 0 & 0 & 0 & 0 \\ \nu_1 & 0 & \nu_2 & 0 \end{bmatrix}, C = \begin{bmatrix} 0 & 0 & 0 \\ \gamma & 0 & 0 \\ 0 & 0 & 0 \end{bmatrix},$$

and

$$D = \begin{bmatrix} -\mu_2 - \sigma_2 & 0 & 0 \\ 0 & -\mu_3 - \gamma_1 - \gamma_2 & 0 \\ 0 & \gamma & -\mu_3 - \sigma_3 \end{bmatrix}.$$

To show that matrices A and $D - CA^{-1}B$ are Metzler stable, we need to demonstrate that all their off-diagonal elements are non-negative. Since the off-diagonal elements of A are β_1 and 0, both of which are non-negative, we conclude that matrix A is Metzler stable.

Next, matrix $D - CA^{-1}B$ can be calculated as follows:

$$CA^{-1}B = \begin{bmatrix} \frac{\tau_1 \theta_1}{\mu_1} & 0 & \frac{\tau_2 \theta_1}{\mu_1} \\ 0 & 0 & 0 \\ 0 & \gamma & -\mu_2 - \sigma_2 \end{bmatrix}.$$

Subtracting $CA^{-1}B$ from D gives

$$D - CA^{-1}B = \begin{bmatrix} 0 & 0 & 0 \\ 0 & -\mu_1 - \sigma_1 & 0 \\ 0 & 0 & -\mu_2 - \gamma - \sigma_2 \end{bmatrix}.$$

Since the eigenvalues of the Matrix B are $\lambda_1 = -\mu_3$, $\lambda_2 = -\mu_2$, $\lambda_3 = -\mu_1$, $\lambda_4 = -(\mu_3 + \gamma_3)$, and $\lambda_5 = -(\beta_3 + \mu_1)$ and the off-diagonal elements of $D - CA^{-1}B$ are all 0, which are non-negative, thus matrix $D - CA^{-1}B$ is also Metzler stable. Since both matrices A and $D - CA^{-1}B$ have non-negative off-diagonal elements, they are Metzler stable. Thus, B_2 is also Metzler stable. Therefore, the rabies free equilibrium point of the model system (5) is globally asymptotically stable if $\mathcal{R}_0 < 1$ and unstable otherwise.

3.3.2. Rabies Persistence Equilibrium Point (RPEP)

The endemic equilibrium point is the steady state where rabies is present in humans, free-range dogs, and domestic dogs. To find this point, we set the equations of the model system (5) to zero and solve the resulting system simultaneously. The state variables for each compartment are represented by

$$\text{RPEP} (S_H^*, E_H^*, I_H^*, R_H^*, S_F^*, E_F^*, I_F^*, S_D^*, E_D^*, I_D^*, R_D^*, M^*)$$

such that

$$\left. \begin{aligned} R_H^* &= \frac{\beta_2 (\sigma_1 + \mu_1) I_H^*}{\beta_1 (\beta_3 + \mu_1)}, \\ I_H^* &= \frac{\beta_1 (\beta_3 + \mu_3) (\sigma_1 + \mu_1)^2 (\beta_1 + \beta_2 + \beta_3) \mu_1 + \beta_1 \beta_3 (\sigma_1 + \mu_1)^2}{(\sigma_1 + \mu_1)^2 ((\beta_1 + \beta_2 + \beta_3) \mu_1 + \beta_1 \beta_3)} \\ &\quad - \frac{\beta_1 (\beta_3 + \mu_3) (\sigma_1 + \mu_1)^2 \beta_3 - \theta_1 (\beta_3 + \mu_3) (\sigma_1 + \mu_1)^2}{(\sigma_1 + \mu_1)^2 ((\beta_1 + \beta_2 + \beta_3) \mu_1 + \beta_1 \beta_3)}, \\ E_H^* &= \frac{(\sigma_1 + \mu_1) I_H^*}{\beta_1}, \\ S_H^* &= \frac{\beta_3 \beta_2 (\sigma_1 + \mu_1) I_H^*}{\beta_1 (\beta_3 + \mu_1) \mu_1} - \frac{(\mu_1 + \beta_1 + \beta_2) (\sigma_1 + \mu_1) I_H^*}{\beta_1 \mu_1} + \frac{\theta_1}{\mu_1} \end{aligned} \right\}.$$

Re-writing Eq. (25) as

$$(R_0 - 1)(R_0 - R_{33} - R_{55} + 1) + (1 - R_{33})(1 - R_{55}) - R_{35}R_{53} = 0, \quad (30)$$

where R_{33} , R_{55} , R_{35} , and R_{53} are defined in Eq. (24), we get

$$\left. \begin{aligned} I_D^* &= \frac{\gamma_1 \psi_1 I_F^* (1 + \rho_2)(1 + \rho_3) M^* + \gamma_1 \psi_3 M^* (1 + \rho_1)(1 + \rho_2)}{(\mu_3 + \gamma_1 + \gamma_2)^2 - \gamma_1 \psi_2 (1 + \rho_1)(1 + \rho_3) M^* (\mu_3 + \gamma_1 + \gamma_2)}, \\ E_D^* &= \frac{(\mu_3 + \sigma_3) I_D^*}{\gamma_1}, \quad R_D^* = \frac{\gamma_2 (\mu_3 + \sigma_3) I_D^*}{\gamma_1 (\mu_3 + \gamma_3)}, \end{aligned} \right\}$$

$$\left. \begin{aligned} S_D^* &= \frac{\gamma_3 (\mu_3 + \sigma_3) I_D^*}{\mu_3 \gamma_1} - \frac{(\mu_3 + \gamma_1 + \gamma_2) \gamma_2 (\mu_3 + \sigma_3) I_D^*}{\gamma_1 (\mu_3 + \gamma_3) \mu_3} + \frac{\theta_3}{\mu_3}, \quad E_F^* = \frac{(\mu_2 + \sigma_2) I_F^*}{\gamma}, \\ S_F^* &= \frac{\theta_2}{\mu_2} - \frac{(\mu_2 + \gamma) (\mu_2 + \sigma_2) I_F^*}{\gamma \mu}, \quad M^* = \frac{\nu_3 I_D^* + \nu_2 I_F^* + \nu_1 I_H^*}{\mu_4}, \end{aligned} \right\}$$

where

$$\theta_2 = \frac{(\mu_2 + \gamma) \mu_2 (1 + (R_0 - 1)) (1 + \rho_1) \mu_3 (\mu_2 + \sigma_2)}{[\mu_3 (1 + \rho_2) (1 + \rho_1) (\mu_3 + \sigma_3) (\mu_3 + \gamma_1 + \gamma_2) (1 + (R_0 - 1)) - \theta_3 \gamma_1 (\psi_2 (1 + \rho_1) \mu_3 + \psi_1 (1 + \rho_2))] \gamma \kappa_1} \\ \times [(1 + \rho_2) (\mu_3 + \sigma_3) (\mu_3 + \gamma_1 + \gamma_2) (1 + (R_0 - 1)) - \theta_3 \psi_2 \gamma_1],$$

$$\theta_3 = \frac{[-\mu_2 (\mu_2 + \sigma_2) (\mu_2 + \gamma) (1 + (R_0 - 1)) + \gamma \kappa_1 \theta_2] (1 + (R_0 - 1)) (1 + \rho_1) \mu_3 (1 + \rho_2) (\mu_3 + \sigma_3) (\mu_3 + \gamma_1 + \gamma_2)}{[(-\mu_2 (\mu_2 + \sigma_2) (\mu_2 + \gamma) (1 + (R_0 - 1)) + \gamma \kappa_1 \theta_2) (1 + \rho_1) \psi_2 \mu_3 + \gamma \kappa_1 \theta_2 \psi_1 (1 + \rho_2)] \gamma_1}.$$

The endemic equilibrium point of the rabies disease persists when I_H , I_F , I_D , $M > 0$ and $\mathcal{R}_0 \geq 1$, as summarized in Theorem 4.

Theorem 4. *The system (5) has a unique endemic equilibrium RPEP if $\mathcal{R}_0 \geq 1$ and I_H , I_F , I_D , $M > 0$.*

4. Quantitative analysis

In this study, we create artificial data sets that represents the dynamics of infectious diseases and estimate model parameters using the least squares technique. Baseline parameter values Θ_i of the rabies model from the literature are used to numerically solve a non-linear deterministic model (5) in the Matlab environment, generating synthetic datasets at each time t_i . Initial conditions for the number of susceptible, exposed infected, and recovered humans, free range and Domestic dogs are also provided.

4.1. Parameter estimation and model fitting

In order to generate the rabies model-predicted number of infected individuals $RD(t_i; \Theta_i)$ dataset at time t_i for a given parameter vector Θ_i , we added random Gaussian noise $\eta_i(t_i; \Theta_i)$ measurements to the data simulate real-world dynamics, where measurement errors are common. Thus, the observed dependent data were given as

$$I(t_i; \Theta_i) = RD(t_i; \Theta_i) + \eta_i(t_i; \Theta_i) \quad \text{for each time } t_i \in [1, n], \quad (31)$$

where n is the number of data points. The objective function quantifies the difference between the model's predictions $I(t_i; \Theta_i)$ and the estimated data $I_{\text{estimated},i}$. We define the objective function $J(\Theta_i)$ as the sum of squared differences between model predictions and estimated dataset as

$$J(\Theta_i) = \sum_{i=1}^{33} a_i (I(t_i; \Theta_i) - I_{\text{estimated},i})^2, \quad (32)$$

where $I_{\text{estimated},i}$ is the estimated number of infected rabies individuals at time t_i . The term

$$(I(t_i; \Theta_i) - I_{\text{estimated},i})^2$$

represents the squared difference between the model-predicted value $I(t_i; \Theta_i)$ and the estimated value $I_{\text{estimated},i}$ at time t_i ; a_i typically represents the weighting or importance assigned to each term in the summation. The goal is to find the parameter vector $\hat{\Theta}_i$ that minimizes the objective function $J(\Theta_i)$ given by

$$\hat{\Theta}_i = \arg \min J(\Theta_i). \quad (33)$$

The expression indicates that $\hat{\Theta}_i$ is the parameter vector that optimally fits the model to the estimated data by minimizing the objective function $J(\Theta_i)$. The symbol $\arg \min$ is used to find the argument (in this case, Θ_i) that minimizes the function $J(\Theta_i)$. To find the parameter value Θ_i , we apply partial derivatives on Eq. (5) with respect to each of the 33 parameters represented by Θ_i such that

$$\frac{\partial J(\Theta_i)}{\partial \Theta_i} = \sum_{i=1}^{33} 2 (I(t_i; \Theta_i) - I_{\text{estimated},i}) \frac{\partial (I(t_i; \Theta_i))}{\partial \Theta_i} = 0 \text{ for } i = 1, 2, \dots, 33, \quad (34)$$

where (see Table 1)

$$\Theta_i = \rho_1, \rho_2, \rho_3, \theta_1, \tau_1, \tau_2, \tau_3, \beta_1, \beta_2, \beta_3, \mu_1, \sigma_1, \theta_2, \gamma, \kappa_1, \kappa_2, \kappa_3, \sigma_2, \mu_2, \theta_3, \psi_1, \psi_2, \psi_3, \sigma_3, \gamma_1, \gamma_2, \gamma_3, \mu_3, \nu_1, \nu_2, \nu_3, \mu_4, C.$$

Table 1: Estimated model parameters (Year⁻¹), initial guess for parameters (Year⁻¹) and their respective source.

Parameters	Baseline value	Source	Estimated value	Mean (μ) and std (σ)
θ_1	2000	(Estimated)	1993.382113	$\mathcal{N}(1996.691056 \ 4.4679553)$.
τ_1	0.0004	[33]	0.000405	$\mathcal{N}(0.000402 \ 4 \times 10^{-6})$.
τ_2	0.0004	[33]	0.000604	$\mathcal{N}(0.000502 \ 1.44 \times 10^{-4})$.
τ_3	[0.0003 0.0100]	(Estimated)	0.000303	$\mathcal{N}(0.000302 \ 2 \times 10^{-6})$.
β_1	$\frac{1}{6}$	[34, 33]	0.165581	$\mathcal{N}(0.166124 \ 7.68 \times 10^{-4})$.
β_2	[0.54 1]	[34, 13]	0.540487	$\mathcal{N}(0.5402435 \ 3.7815 \times 10^{-4})$.
β_3	1	(Estimated)	0.999301	$\mathcal{N}(0.9996505 \ 1.6521 \times 10^{-4})$.
μ_1	0.0142	[35, 36]	0.014417	$\mathcal{N}(0.014309 \ 1.53 \times 10^{-4})$.
σ_1	1	[34, 13]	1.006332	$\mathcal{N}(1.03166 \ 4.47 \times 10^{-3})$.
θ_2	1000	(Estimated)	1004.12044	$\mathcal{N}(1002.060222 \ 2.913594)$.
κ_1	0.00006	(Estimated)	0.000020	$\mathcal{N}(0.000040 \ 2.8 \times 10^{-5})$.
κ_2	0.00005	(Estimated)	0.000081	$\mathcal{N}(0.000066 \ 2.2 \times 10^{-5})$.
κ_3	[0.00001 0.00003]	(Estimated)	0.000040	$\mathcal{N}(0.000025 \ 2.1 \times 10^{-5})$.
γ	$\frac{1}{6}$	[34, 33, 13]	0.166374	$\mathcal{N}(0.166520 \ 2.07 \times 10^{-4})$.
σ_2	0.09	[34, 37]	0.089556	$\mathcal{N}(0.089778 \ 3.14 \times 10^{-4})$.
μ_2	0.067	(Estimated)	0.066268	$\mathcal{N}(0.066634 \ 1.58 \times 10^{-4})$.
θ_3	1200	(Estimated)	1203.844461	$\mathcal{N}(1201.922230 \ 2.718444)$.
ψ_1	0.0004	[38, 37]	0.000077	$\mathcal{N}(0.000238 \ 2.28 \times 10^{-4})$.
ψ_2	0.0004	[39]	0.000066	$\mathcal{N}(0.000233 \ 2.36 \times 10^{-4})$.
ψ_3	0.0003	(Estimated)	0.000030	$\mathcal{N}(0.0003 \ 1.91 \times 10^{-4})$.
μ_3	0.067	(Estimated)	0.080129	$\mathcal{N}(0.073565 \ 8.056 \times 10^{-3})$.
σ_3	0.08	[34]	0.091393	$\mathcal{N}(0.085697 \ 8.056 \times 10^{-3})$.
γ_1	$\frac{1}{6}$	[34, 33]	0.172489	$\mathcal{N}(0.169578 \ 4.117 \times 10^{-3})$.

Continued on next page

Table 1 – Continued from previous page

Parameters	Baseline value	Source	Estimated value	Mean (μ) and std (σ)
γ_2	0.09	[34]	0.090308	$\mathcal{N}(0.090154 \ 2.18 \times 10^{-4})$.
γ_3	0.05	(Estimated)	0.050128	$\mathcal{N}(0.050128 \ 9.1 \times 10^{-5})$.
ν_1	0.001	(Estimated)	0.001958	$\mathcal{N}(0.001479 \ 6.77 \times 10^{-4})$.
ν_2	0.006	(Estimated)	0.008971	$\mathcal{N}(0.007485 \ 2.101 \times 10^{-3})$.
ν_3	0.001	(Estimated)	0.005735	$\mathcal{N}(0.003367 \ 3.3348 \times 10^{-3})$.
μ_4	0.08	(Estimated)	0.080625	$\mathcal{N}(0.080313 \ 4.42 \times 10^{-4})$.
ρ_1	10	[40]	9.920733	$\mathcal{N}(9.960366 \ 5.605 \times 10^{-2})$.
ρ_2	8	(Estimated)	8.116421	$\mathcal{N}(8.058211 \ 8.2322 \times 10^{-2})$.
ρ_3	15	(Estimated)	14.917005	$\mathcal{N}(14.958502 \ 5.8686 \times 10^{-2})$.
C	0.003 (PFU)/mL	(Estimated)	0.003011	$\mathcal{N}(0.003005 \ 8.0000 \times 10^{-6})$.

4.2. Parameter sensitivity analysis

For the modeling uncertainty and parameter estimation of rabies transmission global sensitivity analysis (GSA), we employed LHS-PRCC to analyze uncertainty, specifically in the context of a model with 33 parameters (referred to as model (5)). The aim is to identify the key factors influencing the transmission of a new infection under a specific intervention, following the approach outlined in reference [36]. This approach involved using LHS to sample the parameters that contribute to the variable \mathcal{R}_0 and calculating Partial Rank Correlation Coefficients (PRCC) for these parameters, as defined in Eq. (35). We conducted a total of 1000 simulations for each LHS run. Our parameter sampling was based on a uniform distribution, treating the model parameters as input variables, and \mathcal{R}_0 as the output variable. Larger absolute PRCC values indicate a more substantial influence of a parameter on \mathcal{R}_0 . If the p -value exceeds 0.05, it is assumed that a parameter is not statistically significant for \mathcal{R}_0 . Positive values denote positive correlations, negative values signify negative correlations, and values within the range of -0.2 to +0.2 represent weak or negligible correlations. PRCC values greater than +0.6 or less than -0.6 indicate strong positive or strong negative correlations, while values within the range of $0.2 < \text{PRCC} < 0.6$ or $-0.6 < \text{PRCC} < -0.2$ represent moderate positive or moderate negative correlations, respectively.

The PRCC between parameter y_i and output x_j , controlling for the effects of other variables Z , is then computed as

$$\text{PRCC}(y_i, x_j|Z) = \frac{\text{cov}(X, Y)}{\sigma_X \sigma_Y} = \frac{\text{Corr}(y_i, x_j|Z)}{\sqrt{\text{Corr}(y_i, y_i|Z) \times \text{Corr}(x_j, x_j|Z)}}, \quad (35)$$

where X is the matrix of model outputs (e.g., disease incidence or prevalence), Y is the matrix of model parameters (e.g., transmission rates, recovery rates), Z is the matrix of other relevant variables, $\text{cov}(X, Y)$ is the covariance between the model output (X) and the input parameter (Y), and σ_X and σ_Y are the standard deviations of X and Y , respectively.

Once PRCC and LHS values are computed for each parameter, they were plotted against the model output to visualize their impact. This visualization helps identify which parameters have the most significant influence on the model output and how changes in those parameters affect the model behavior. Additionally, these techniques aid in obtaining solutions by guiding parameter estimation processes and improving model calibration and validation.

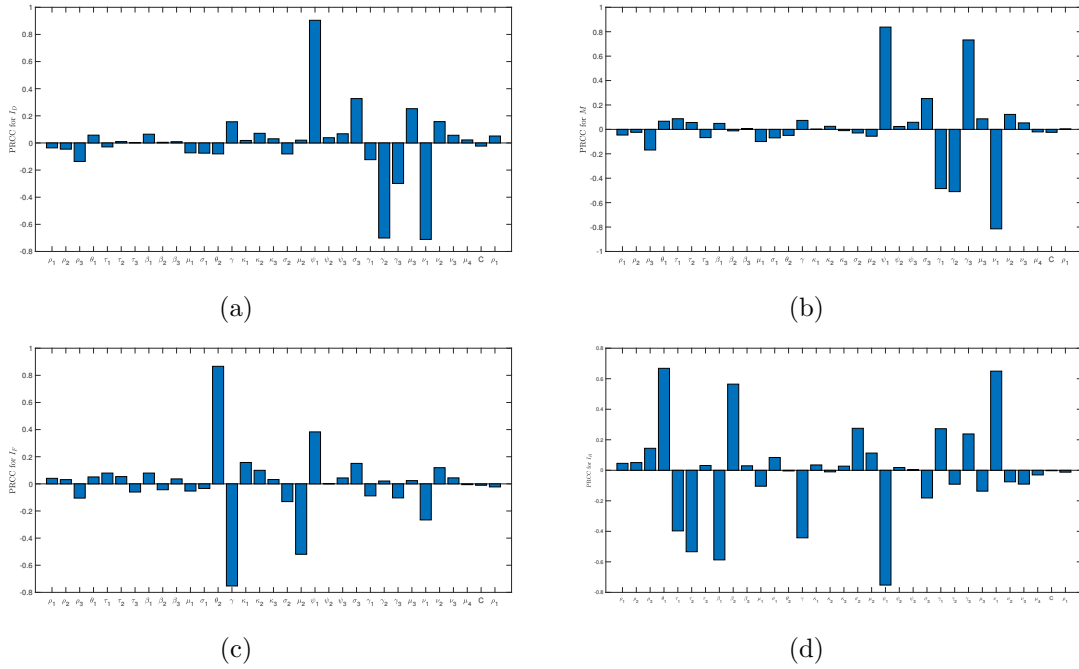


Figure 2: The sensitivity analysis of Rabies model dynamics involved 1000 simulations employing Latin Hypercube Sampling (LHS). The analysis evaluated Partial Rank Correlation Coefficients (PRCCs) concerning (a) domestic dogs, (b) Environment, (c) Free-range dogs, and (d) Human population, respectively.

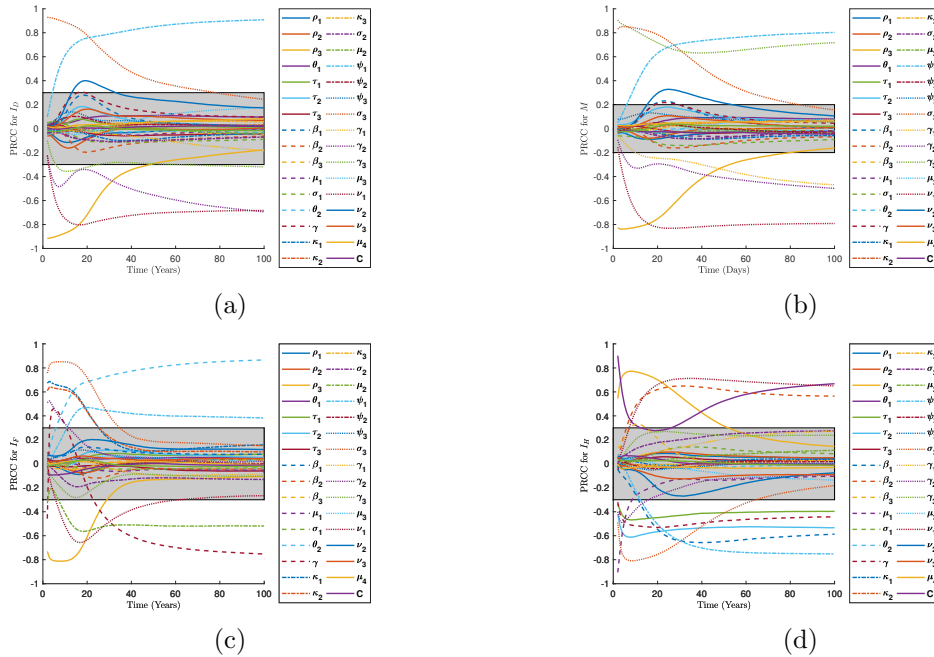


Figure 3: A visual representation showcasing the evolution of parameter sensitivity throughout the progression of the system dynamics. PRCC values over time span of 100 years with respect to (a) domestic dogs, (b) Environment, (c) Free-range dogs, and (d) Human population.

The PRCC results provide insights into the impact of each parameter on the model and its associated

uncertainty. Parameters with PRCC values close to zero, or equal to zero, are considered statistically insignificant. Fig. 2 indicates that $\psi_1, \psi_2, \psi_3, \tau_1, \tau_2, \tau_3, \kappa_1, \kappa_2,$ and κ_3 have positive correlation with the transmission dynamics of rabies based on the model solution computed in Eq. (35), while $\rho_1, \rho_2, \rho_3, \beta_1, \beta_2, \beta_3, \mu_1, \sigma_1, \sigma_2, \mu_2, \theta_3, \psi_1, \psi_2, \psi_3, \sigma_3, \gamma_1, \gamma_2, \gamma_3, \mu_3,$ and C have negative correlation with the transmission dynamics of rabies. Fig. 3 illustrates the sensitivity of PRCC values across the entire time interval of the model simulation. It assesses significance and demonstrates how the sensitivity of each parameter influences the dynamics of the model system. This suggests that, to control rabies in humans and dogs, more efforts should be directed to reduce the rate of infections by intervening the transmission and control of the contact rate.

4.3. Numerical simulation

Due to the resource-intensive nature of individually solving for 33 parameters, we employed the MATLAB built-in function `fminsearch`, which leverages the Nelder-Mead simplex algorithm [41] to identify local minima for the residual sum of squares as presented in Eq. (34). Our choice of initial parameter values was guided by the criteria established during the qualitative analysis along with the initial conditions $S_H(0) = 142000, E_H(0) = 40, I_H(0) = 0, R_H(0) = 0, S_D(0) = 15000, E_D(0) = 25, I_D(0) = 0, R_D(0) = 0, S_F(0) = 12500, E_F(0) = 20, I_F(0) = 0, M(0) = 90$. The estimated parameter values in Table 1 were then applied to model the data, and the outcomes are presented in Figures 4–7.

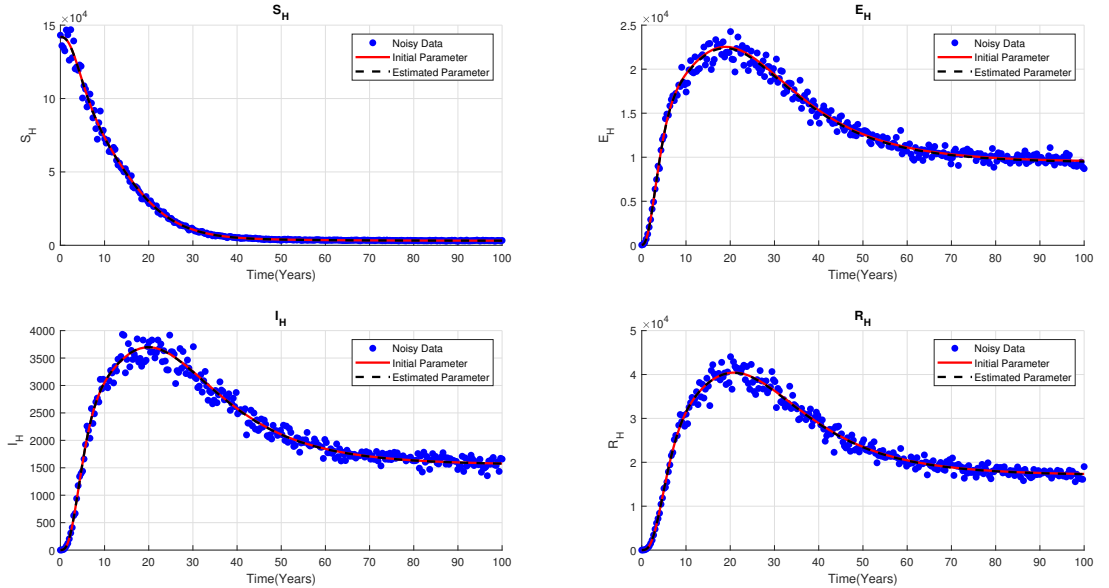


Figure 4: Model fitting and scatter plot with corresponding parameter estimation with standard deviation $\sigma=0.05$ and Confidence interval (C.I.)=95% for human population.

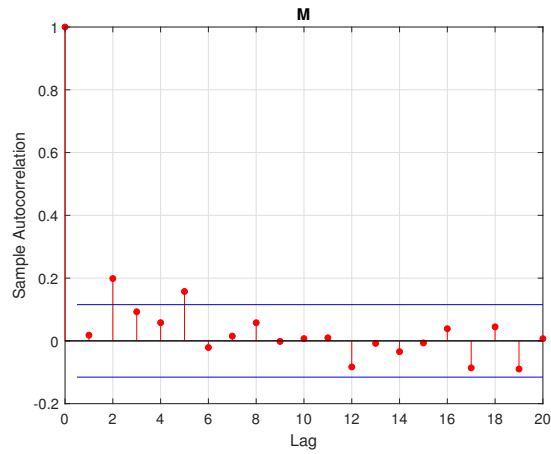


Figure 5: The sample autocorrelation of the residuals in relation to environment indicating the lack of significance at the 5% level.

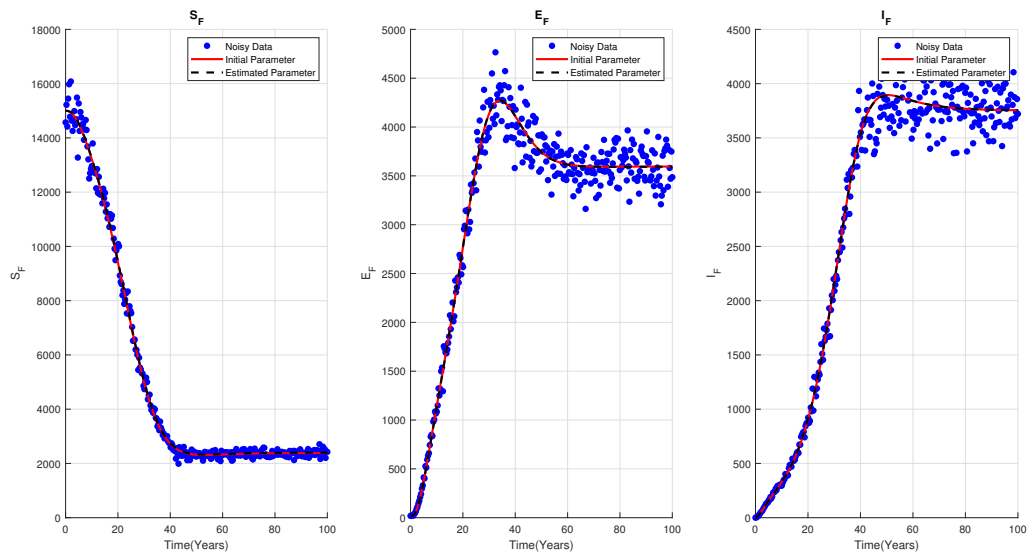


Figure 6: Model fitting and scatter plot with corresponding parameter estimation with standard deviation $\sigma=0.05$ and Confidence interval (C.I.)=95% for free range dogs.

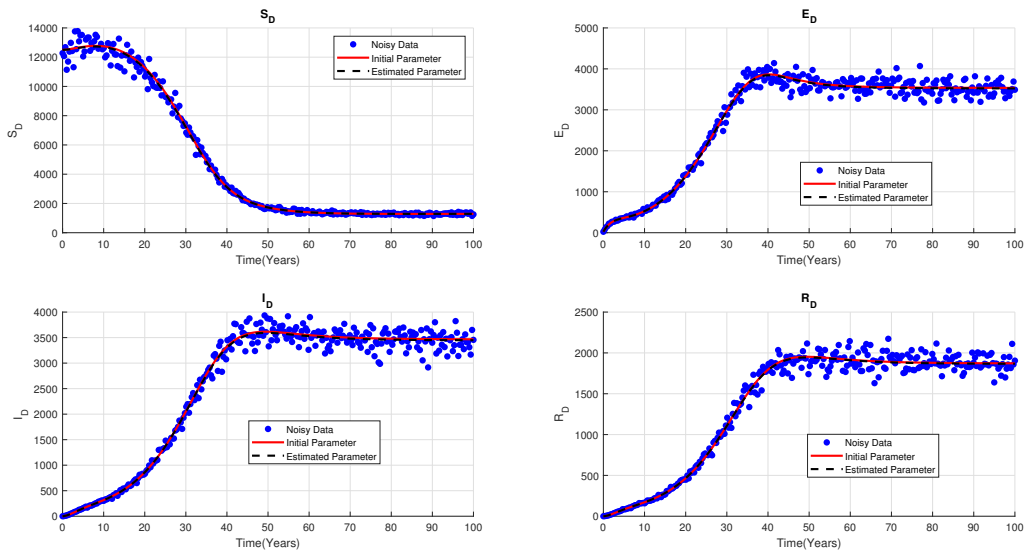


Figure 7: Model fitting and scatter plot with corresponding parameter estimation with standard deviation $\sigma=0.05$ and Confidence interval (C.I.)=95% for domestic dogs.

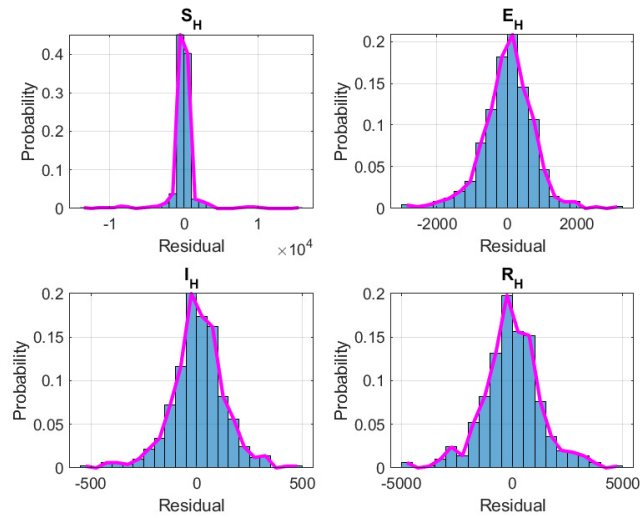


Figure 8: Normal distribution of the rabies model variable with standard deviation $\sigma=0.05$ and Confidence interval (C.I.)=95% for human population.

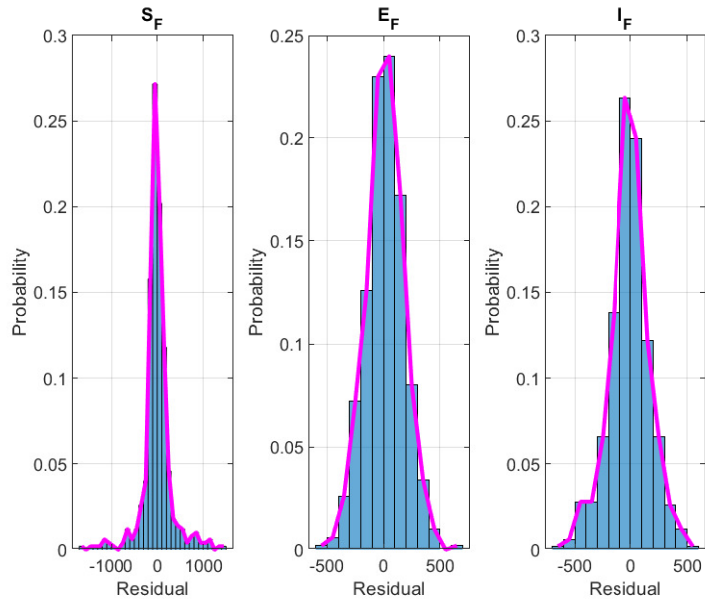


Figure 9: Normal distribution of the rabies model variable with standard deviation $\sigma=0.05$ and Confidence interval (C.I.)=95% for free-range dogs population.

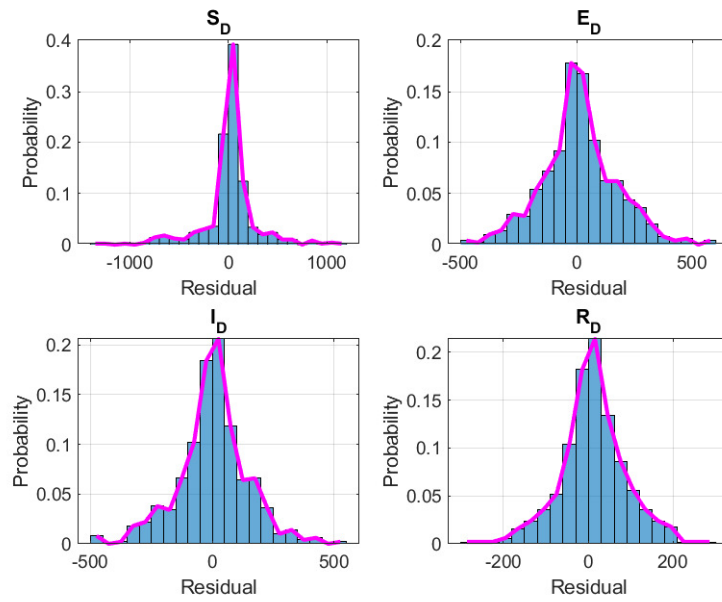


Figure 10: Normal distribution of the rabies model variable with standard deviation $\sigma=0.05$ and Confidence interval (C.I.)=95% for domestic dogs population.

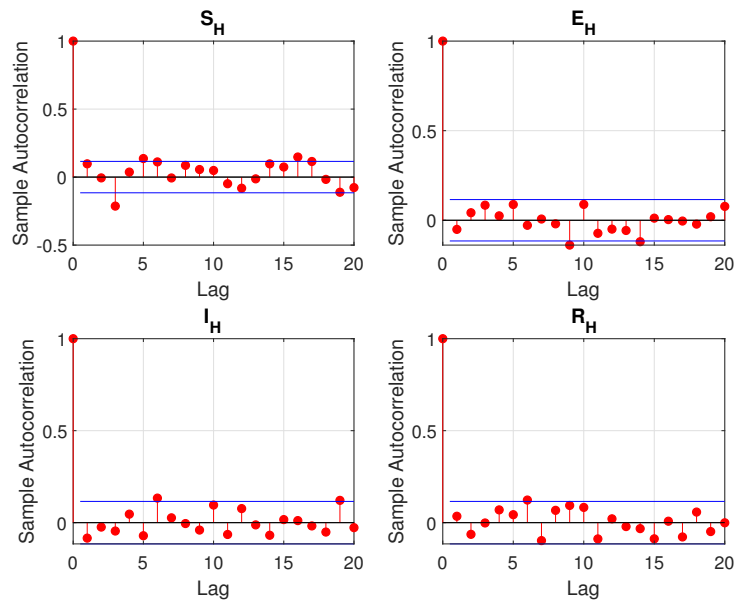


Figure 11: The sample autocorrelation of the residuals in relation to human population indicating the lack of significance at the 5% level.

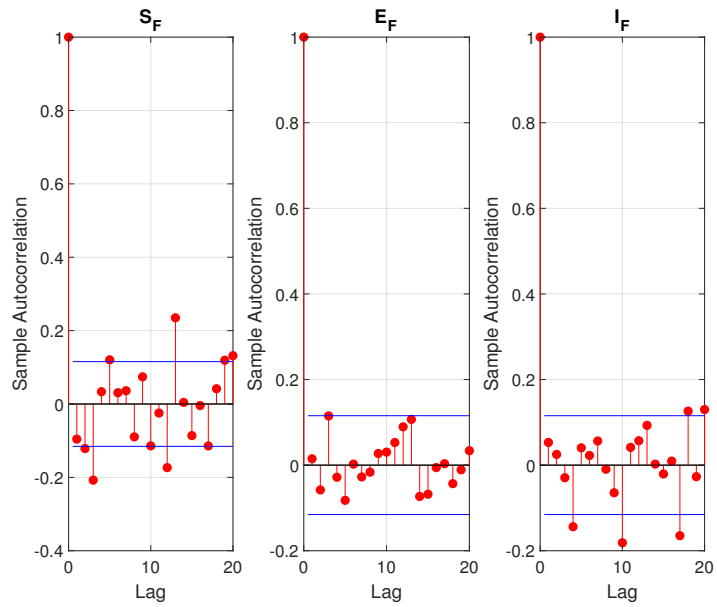


Figure 12: The sample autocorrelation of the residuals in relation to domestic dogs indicating the lack of significance at the 5% level.

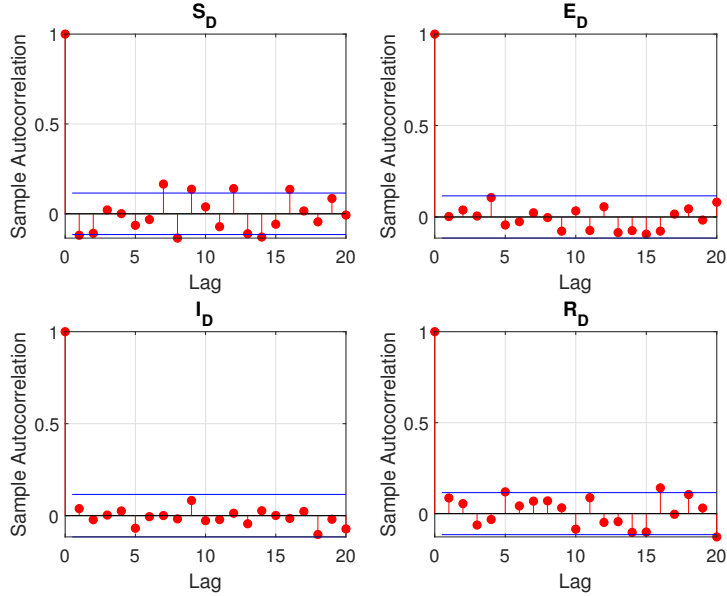


Figure 13: The sample autocorrelation of the residuals in relation to free range indicating the lack of significance at the 5% level.

5. Discussion

Figures 8–10 illustrate the histogram of residuals, which provide insight into the consistency between the proposed model fitting and the estimated parameter values, indicating that they stem from the same probability distribution function. By examining the distribution of residuals, which represent the differences between observed data and model predictions, we can assess how effectively the model captures the underlying dynamics of rabies transmission. Meanwhile, Figs. 11–13 show an autocorrelation between 0.2 and -0.2, implying a moderate to weak correlation between consecutive residuals. This suggests that the errors in the model predictions are relatively independent of each other over time, which can be interpreted as a desirable property indicating that the model adequately captures the underlying dynamics without systematic biases or trends in the residuals.

However, the spread of infectious diseases among human and dog populations often results in a dynamic interplay between the number of susceptible individuals and the number of infected individuals. In particular, Figs. 4–13 show trends for humans, free-range and domestic dog populations. The data presented in these figures suggest that as the number of infections increases, the number of susceptible individuals decreases towards a non-negative constant value. This phenomenon can be explained by the increased contact rate between infectious and susceptible compartments.

6. Conclusion

In this study, we developed and analyzed a deterministic model to estimate parameters and assess uncertainty in the transmission dynamics of rabies in humans and dogs. Data were generated by adding random Gaussian noise to a real world data, and parameter values were estimated using the non-linear least squares method. The basic reproduction number \mathcal{R}_0 was derived using the next-generation matrix approach. We determined model equilibria and found that the rabies-free equilibrium is globally asymptotically stable when \mathcal{R}_0 is less than one, and the rabies-endemic equilibrium is globally stable when \mathcal{R}_0 is greater than or equal to one. Latin Hypercube and Partial Rank Correlation Coefficient analyses were employed to identify which parameters positively or negatively affect model outputs. Sensitivity analysis revealed that contact rates between humans and dogs contribute to an increase in average new rabies infections in the entire population.

CRedit Authorship Contribution Statement

Mfano Charles: Writing – original draft, Software, Methodology, Formal analysis, Conceptualization. Sayoki G. Mfinanga: Writing – review & editing, Supervision, Methodology, Data curation, Conceptualization. G. A. Lyakurwa: Writing – review & editing, Supervision. Delfim F. M. Torres: Writing – review & editing, Supervision, Methodology. Verdiana G. Masanja: Writing – review & editing.

Funding Statement

Torres is supported by the Portuguese Foundation for Science and Technology (FCT) and CIDMA, project UIDB/04106/2020.

Declaration of Competing Interest

The authors declare that they have no known competing financial interests or personal relationships that could have appeared to influence the work reported in this paper.

Acknowledgments

The authors would like to extend their gratitude to the handling editor and the referee for their valuable input, which significantly contributed to enhancing the quality of this manuscript. Furthermore, we wish to acknowledge The Nelson Mandela African Institution of Science and Technology (NM-AIST) and the College of Business Education (CBE) for providing a conducive environment during the writing of this manuscript.

Data Availability

The data used in this study are included in the manuscript.

References

- [1] D. K. Bonilla-Aldana, S. D. Jimenez-Diaz, J. J. Barboza, A. J. Rodriguez-Morales, Mapping the spatiotemporal distribution of bovine rabies in Colombia, 2005–2019, *Tropical Medicine and Infectious Disease* 7 (12) (2022) 406.
- [2] C. B. Barecha, F. Girzaw, R. V. Kandi, M. Pal, Epidemiology and public health significance of rabies, *Perspect Clin Res* 5 (1) (2017) 55–67.
- [3] J. M. Kabeto, Y. T. Tewabe, A. W. Haile, W. Gemechu, Rabies: A neglected zoonotic disease and its public health concern in Ethiopia, *Journal of Zoonotic Diseases* 5 (4) (2021) 1–11.
- [4] S. Kavosian, R. Behzadi, M. Asouri, A. A. Ahmadi, M. Nasirikenari, A. Salehi, et al., Comparison of rabies cases received by the shomal Pasteur Institute in Northern Iran: a 2-year study, *Global Health, Epidemiology and Genomics* 2023 (2023).
- [5] T. Lembo, K. Hampson, M. T. Kaare, E. Ernest, D. Knobel, R. R. Kazwala, D. T. Haydon, S. Cleaveland, The feasibility of canine rabies elimination in Africa: dispelling doubts with data, *PLoS Neglected Tropical Diseases* 4 (2) (2010) e626.
- [6] S. Rocha, S. de Oliveira, M. B. Heinemann, V. Gonçalves, Epidemiological profile of wild rabies in Brazil (2002–2012), *Transboundary and Emerging Diseases* 64 (2) (2017) 624–633.
- [7] L. H. Taylor, L. H. Nel, Global epidemiology of canine rabies: past, present, and future prospects, *Veterinary Medicine: Research and Reports* (2015) 361–371.

- [8] S. C. Marsden, C. R. Cabanban, Rabies: A significant palliative care issue, *Progress in Palliative Care* 14 (2) (2006) 62–67.
- [9] T. P. Monath, Vaccines against diseases transmitted from animals to humans: a one health paradigm, *Vaccine* 31 (46) (2013) 5321–5338.
- [10] J. Maki, A.-L. Guiot, M. Aubert, B. Brochier, F. Cliquet, C. A. Hanlon, R. King, E. H. Oertli, C. E. Rupprecht, C. Schumacher, et al., Oral vaccination of wildlife using a vaccinia–rabies-glycoprotein recombinant virus vaccine (RABORAL V-RG[®]): a global review, *Veterinary Research* 48 (2017) 1–26.
- [11] A. Velasco-Villa, L. E. Escobar, A. Sanchez, M. Shi, D. G. Streicker, N. F. Gallardo-Romero, F. Vargas-Pino, V. Gutierrez-Cedillo, I. Damon, G. Emerson, Successful strategies implemented towards the elimination of canine rabies in the western hemisphere, *Antiviral Research* 143 (2017) 1–12.
- [12] C. M. Gossner, A. Mailles, I. Aznar, E. Dimina, J. E. Echevarría, S. L. Feruglio, H. Lange, F. P. Maraglino, P. Parodi, J. Perevoscikovs, et al., Prevention of human rabies: a challenge for the European Union and the European Economic Area, *Eurosurveillance* 25 (38) (2020) 2000158.
- [13] S. Abdulmajid, A. S. Hassan, Analysis of time delayed rabies model in human and dog populations with controls, *Afrika Matematika* 32 (5-6) (2021) 1067–1085.
- [14] Y. Amoako, P. El-Duah, A. Sylverken, M. Owusu, R. Yeboah, R. Gorman, T. Adade, J. Bonney, W. Tasiame, K. Nyarko-Jectey, et al., Rabies is still a fatal but neglected disease: a case report, *Journal of Medical Case Reports* 15 (1) (2021) 1–6.
- [15] F. M. Abrahamian, C. E. Rupprecht, Rhabdovirus: Rabies. In: *Viral Infections of Humans: Epidemiology and Control*, Springer, 2022, pp. 1–49.
- [16] S. Ruan, Modeling the transmission dynamics and control of rabies in China, *Mathematical Biosciences* 286 (2017) 65–93.
- [17] A. A. Ayoade, O. J. Peter, T. A. Ayoola, S. Amadiogwu, A. Victor, A saturated treatment model for the transmission dynamics of rabies, *Malaysian Journal of Computing* 4 (1) (2019) 201–213.
- [18] M. Chapwanya, P. Dumani, Environment considerations on the spread of rabies among African wild dogs (*lycaon pictus*) with control measures, *Mathematical Methods in the Applied Sciences* 45 (8) (2022) 4124–4139.
- [19] H. Kadowaki, K. Hampson, K. Tojinbara, A. Yamada, K. Makita, The risk of rabies spread in Japan: a mathematical modelling assessment, *Epidemiology & Infection* 146 (10) (2018) 1245–1252.
- [20] A. A. Ayoade, M. O. Ibrahim, Modeling the dynamics and control of rabies in dog population within and around Lagos, Nigeria, *The European Physical Journal Plus* 138 (5) (2023) 397.
- [21] A. M. Tulu, P. R. Koya, The impact of infective immigrants on the spread of dog rabies, *American Journal of Applied Mathematics* 5 (3) (2017) 68.
- [22] B. Pantha, S. Giri, H. R. Joshi, N. K. Vaidya, Modeling transmission dynamics of rabies in Nepal, *Infectious Disease Modelling* 6 (2021) 284–301.
- [23] O. C. Eze, G. E. Mbah, D. U. Nnaji, N. E. Onyiaji, Mathematical modelling of transmission dynamics of rabies virus, *International Journal of Mathematics Trends and Technology* 66 (2020).
- [24] T. T. Ega, L. Luboobi, D. Kuznetsov, A. H. Kidane, Sensitivity analysis and numerical simulations for the mathematical model of rabies in human and animal within and around Addis Ababa, *Asian Journal of Mathematics and Applications* (2015).
- [25] M. Renardy, C. Hult, S. Evans, J. J. Linderman, D. E. Kirschner, Global sensitivity analysis of biological multiscale models, *Current Opinion in Biomedical Engineering* 11 (2019) 109–116.

- [26] B. Gomero, Latin hypercube sampling and partial rank correlation coefficient analysis applied to an optimal control problem, Ph.D. thesis, University of Tennessee (2012). https://trace.tennessee.edu/utk_gradthes/1278
- [27] J. P. LaSalle, Stability theory and invariance principles. In: Dynamical Systems, Elsevier, 1976, pp. 211–222.
- [28] H. M. Yang, The basic reproduction number obtained from Jacobian and next generation matrices—a case study of dengue transmission modelling, *Biosystems* 126 (2014) 52–75.
- [29] S. Saha, G. Samanta, Dynamics of an epidemic model under the influence of environmental stress, *Mathematical Biology and Bioinformatics* 16 (2) (2021) 201–243.
- [30] S. Dharmaratne, S. Sudaraka, I. Abeyagunawardena, K. Manchanayake, M. Kothalawala, W. Gunathunga, Estimation of the basic reproduction number (R_0) for the novel coronavirus disease in Sri Lanka, *Virology Journal* 17 (2020) 1–7.
- [31] C. Castillo-Chavez, Z. Feng, W. Huang, On the computation of r and its role on global stability, *Mathematical approaches for emerging and reemerging infectious diseases: an introduction*, 1 (2002) 229.
- [32] J. C. Kamgang, G. Sallet, Computation of threshold conditions for epidemiological models and global stability of the disease-free equilibrium (DFE), *Mathematical Biosciences* 213 (1) (2008) 1–12.
- [33] H. Tian, Y. Feng, B. Vrancken, B. Cazelles, H. Tan, M. S. Gill, Q. Yang, Y. Li, W. Yang, Y. Zhang, et al., Transmission dynamics of re-emerging rabies in domestic dogs of rural China, *PLoS Pathogens* 14 (12) (2018) e1007392.
- [34] J. Zhang, Z. Jin, G.-Q. Sun, T. Zhou, S. Ruan, Analysis of rabies in China: transmission dynamics and control, *PLoS One* 6 (7) (2011) e20891.
- [35] W. H. Organization, et al., Working to overcome the global impact of neglected tropical diseases: first WHO report on neglected tropical diseases, no. WHO/HTM/NTD/2010.1 in WHO Library Cataloguing-in-Publication Data, World Health Organization, 2010.
- [36] W. H. Organization, WHO expert consultation on rabies: second report, Vol. 982, World Health Organization, 2013.
- [37] K. M. Addo, An SEIR mathematical model for dog rabies; case study: Bongo district, Ghana, Ph.D. thesis, Kwame Nkrumah University of Science and Technology, Kumasi (2012).
- [38] K. Hampson, F. Ventura, R. Steenson, R. Mancy, C. Trotter, L. Cooper, B. Abela-Ridder, L. Knopf, M. Ringenier, T. Tenzin, et al., The potential effect of improved provision of rabies post-exposure prophylaxis in gavi-eligible countries: a modelling study, *The Lancet Infectious Diseases* 19 (1) (2019) 102–111.
- [39] D. D. Hailemichael, G. K. Edessa, P. R. Koya, Effect of vaccination and culling on the dynamics of rabies transmission from stray dogs to domestic dogs, *Journal of Applied Mathematics* 2022 (2022).
- [40] S. Ruan, Spatiotemporal epidemic models for rabies among animals, *Infectious Disease Modelling* 2 (3) (2017) 277–287.
- [41] J. C. Lagarias, J. A. Reeds, M. H. Wright, P. E. Wright, Convergence properties of the nelder–mead simplex method in low dimensions, *SIAM Journal on Optimization* 9 (1) (1998) 112–147.